Aerosol and Air Quality Research, 15: 1799–1812, 2015

ISSN: 1680-8584 print / 2071-1409 online
doi: 10.4209/aaqr.2015.05.0363

Two-Years $PM_{2.5}$ Observations at Four Urban Sites along the Coast of Southeastern China

Shui-Ping Wu[1,2*], James Schwab[3], Bing-Yu Yang[2], An Zheng[2], Chung-Shin Yuan[2,4]

[1] *State Key Laboratory of Marine Environmental Science, Xiamen University, Xiamen 361005, China*
[2] *College of Environment and Ecology, Xiamen University, Xiamen 361005, China*
[3] *Atmospheric Sciences Research Center, University at Albany, SUNY, Albany 12203, USA*
[4] *Institute of Environmental Engineering, National Sun Yat-sen University, Kaohsiung 80424, Taiwan*

ABSTRACT

$PM_{2.5}$ samples from four coastal urban sites (Fuzhou, Putian, Quanzhou, and Xiamen) in Southeastern China were collected to analyze their major chemical composition including inorganic ions, organic carbon (OC), elemental carbon (EC), and inorganic elements. Organic matter (OM = 1.6 × OC) was the largest contributor, accounting for 30.2% of $PM_{2.5}$ mass concentration, and followed by sulfate (19.8%), ammonium (10.6%), and nitrate (9.7%), with minor contribution from trace species (5.1%), crustal species (4.7%) and EC (2.9%). Sea-salt and biomass burning potassium together contributed less than 2%. At the four sites, higher $PM_{2.5}$ and its major components were observed in the northeast monsoon season while lower levels were found in the southwest monsoon season. The periodic $PM_{2.5}$ cycle was observed and influenced mainly by rain wash out. However, regular diurnal variations of $PM_{2.5}$ with high concentration during daytime were only observed in summer due to the greater production of sulfate and organic aerosols in spite of the fact that the vertical mixing coefficients were lower during nighttime. The relative contributions of secondary inorganic aerosols (sulfate, nitrate, and ammonium) to $PM_{2.5}$ increased rapidly while the contribution of OM decreased during the haze episodes. The reconstructed visibility using revised IMPROVE method correlated well with the measured values. At Xiamen and Fuzhou sites, the major contributors of light extinction coefficient were ammonium sulfate, ammonium nitrate, OM and coarse mass, and accounted for more than 80% of the light extinction coefficient on average.

Keywords: $PM_{2.5}$; Chemical composition; Temporal variation; Visibility; Southeastern China.

INTRODUCTION

In the last few years, there has been an increasing concern about $PM_{2.5}$ pollution in China's mega cities due to their influences on visibility degradation, adverse health effects, and climate change (Zheng *et al.*, 2005; Sun *et al.*, 2006; Feng *et al.*, 2009; Zhao *et al.*, 2009; Yang *et al.*, 2012; Guo *et al.*, 2014; Huang *et al.*, 2014; Zhang *et al.*, 2015). The reported levels of $PM_{2.5}$ in China's megacities are generally very high compared with internationally accepted health goals. Many studies of $PM_{2.5}$ in China have focused mainly on its chemical composition such as SO_4^{2-}, NO_3^-, NH_4^+, organic carbon (OC), crustal matter and elemental carbon (EC) which are the dominant species (Song *et al.*, 2006; Wang *et al.*, 2006; Yang *et al.*, 2011; Xu *et al.*, 2012; Guo *et al.*, 2014; Huang *et al.*, 2014). Motor vehicles, fossil-fuel combustion, industrial processes, biomass burning and windblown soil dusts are suggested to be the main sources of $PM_{2.5}$ (Yao *et al.*, 2003; Zheng *et al.*, 2005; Song *et al.*, 2006; Wang *et al.*, 2006). Because the ambient concentration and chemical composition of $PM_{2.5}$ are highly dependent on the locations, emission sources, and meteorological conditions, it is necessary to carry out intensive sampling campaigns at many locations and seasons to investigate the factors influencing the chemical components of $PM_{2.5}$ in order to identify their sources and atmospheric formation pathways.

Four urban sites at Xiamen, Quanzhou, Putian and Fuzhou were established along the coast line of Fujian province, China, for this study. These cities are considered the main economic engines of the Western Taiwan Strait Economic Zone (WTSEZ), an association created to facilitate political and economic relationships across the Taiwan Strait, similar to the Pearl River Delta (PRD) and the Yangtze River Delta (YRD) and supported by the Chinese central government., This area has been undergoing accelerated economic growth, urbanization, industrial expansion and population growth. In year 2015. the estimated emissions of SO_2 and NO_x from coal power plants are projected decrease 35.5% and 45.6%,

* Corresponding author.
Tel.: 0086-13400631797
E-mail address: wsp@xmu.edu.cn

respectively, when compared with those in the year of 2009 due to the use of power plant scrubbers; however, the emissions from vehicles are projected to increase 86.5% and 44.3% for SO_2 and NO_x, respectively, due to the rapid urbanization and increase of port cargo transportation and the logistics industries in this coastal urban zone (Lu *et al.*, 2014). To date there are few observational studies on $PM_{2.5}$ and the associated chemical components reported from this area (Hsu *et al.*, 2010; Zhang *et al.*, 2011; Xu *et al.*, 2012; Li *et al.*, 2013a, b).

The WTSEZ's position is in-between the YRD and PRD (Fig. 1), a region influenced by East Asian monsoon circulation patterns characterized by southwesterly winds in summer and northeasterly winds in other three seasons. Both the YRD to the north and the PRD to the south are suffering severe air pollution and the air pollutants from the two regions may contribute to the local air pollution through long-range transport (LRT) (Fu *et al.*, 2008; Feng *et al.*, 2009; Hsu *et al.*, 2010; Henriksson *et al.*, 2011; Yang *et al.*, 2011; Gao *et al.*, 2014; Huang *et al.*, 2014). This coastal urban zone, therefore, is a favorable region to study the regional air pollution and help fill an important data gap (Hsu *et al.*, 2010; Henriksson *et al.*, 2011).

In this study, the daytime (08:00–18:00) and nighttime (18:00–08:00) $PM_{2.5}$ samples were collected separately at the Xiamen, Quanzhou, Putian and Fuzhou urban sites in eight sampling campaigns from November 2011 through July 2013 (Fig. 2).The main objectives of the present study are (i) to provide quantitative information on the concentrations of $PM_{2.5}$ and its major components, and (ii) to investigate the regional air pollution in terms of its chemical characteristics.

EXPERIMENTAL METHODS

Sample Collection and Gravimetric Weighing

$PM_{2.5}$ samples were collected at four urban sampling sites, more specifically the air quality monitoring sites of local government, in Xiamen (XM), Quanzhou (QZ), Putian (PT), and Fuzhou (FZ) of Fujian province in Southeastern China (Fig. 1). The XM site was set on a building roof of Hongwen Primary School, 20 m above the ground (24°28′ 37"N, 118°09′07"E). It is surrounded by residences, light traffic and a few restaurants. The QZ site was situated at the center of Quanzhou urban area. The sampler was placed on the roof of an eight-story building of the Quanzhou City Environmental Protection Bureau, 24 m above the ground (24°53′52"N, 118°35′50"E). The site is surrounded by densely inhabited districts, heavy traffic and few restaurants. The PT site was set on the roof of an office building of Xiuyu District of Putian City, 25 m above the ground (25°19′17"N, 119°06′05"E) in a vast open suburban field. It is surrounded by scattered inhabited residences and light traffic. The FZ site was located on the campus of Fujian Normal University (26°04′31"N, 119°18′55"E). An eight-story office building (24 m above ground) was selected to mount the $PM_{2.5}$ sampler. This site is surrounded by high-rise residential buildings (40–60 m) and busy traffic.

Two $PM_{2.5}$ samplers (TH100-$PM_{2.5}$ cascade impactor, Wuhan Tianhong Instruments, Wuhan, China) were deployed at each site in parallel. The sampling periods of November, January, April and July or June were defined as fall, winter, spring and summer, respectively. Each sampling period was 15 days in which the daytime sampling was from 08:00 to 18:00 and nighttime sampling was from 18:00 to 08:00 the next day. The flow rate was 100 ± 2 L min^{-1} and the particles were trapped using quartz filters (Pallflex 2500QAT-UP, 90 mm) for the analyses of gravimetry, carbon and water soluble ionic species, and polypropylene fiber filters (Tianjin Xinyao Co., Ltd., China, pore size 0.45 μm, 90 mm) for elemental analyses (Xu *et al.*, 2012). All blank quartz filters were prebaked at 600°C for at least 8 h in a muffle furnace to remove impurities, and polypropylene filters were used without further treatment.

$PM_{2.5}$ mass concentration was obtained by gravimetry method with an analytical microbalance (Mettler Toledo AE420, ± 0.01 mg) after being conditioned under constant (20 ± 5°C) and relative humidity (40% ± 5%). Each filter was stored in a separate sealed Petri dish (F-Box, www.bmet.cn) at –20°C before and after sampling. A total of 960 quartz filters and 960 polypropylene filters were collected in this specific sampling protocol. During the sampling periods, the concentrations of criteria air pollutants, such as NO, NO_2, SO_2, and O_3, were available only at the XM and FZ sampling sites from the Fujian Environmental Protection Bureau; meteorological factors, such as temperature, Relative humidity, wind direction, wind speed, atmospheric pressure and rainfall as well as visibility near the two sites (N24.48, E118.08, altitude 139 m; N26.08, E119.28, altitude 85 m) were derived from Weather & Climate website (www.weatherandclimate.info) and atmospheric vertical mixing coefficient (defined as wind speed multiplied by mixing height) were derived from air resources laboratory (www.ready.arl.noaa.gov/Readyamet.php). The average values of temperature (T), relative humidity (RH), wind speed (WS), wind direction (WD), air pressure (P), visibility, vertical mixing coefficient (Mix C) and rainfall (RF) for the eight sampling periods near the XM and FZ sites were summarized and depicted in Figs. 2 and S2.

Chemical Analysis

Carbonaceous species including OC and EC were analyzed by the thermal-optical transmittance analyzer (TOT, Sunset Laboratory Inc., USA) following the temperature program outlined in the NIOSH 5040 method (Birch and Cary, 1996). Around 10% of the samples were randomly selected and measured twice to check the analytical precision. The average relative percentage variations for OC, EC and TC were 4.2 ± 2.9, 10.9 ± 3.9 and 3.1 ± 2.3, respectively (n = 90). Field blanks were used to quantify procedure detection limits. Trace OC (average 0.91 μg C per punch) and EC (average 0.02 μg C per punch) were detected on the field blank filters. The limits of detection (LOD), calculated as three times of the standard deviation (3σ) of the field blanks, were 0.056 and 0.003 μg C m^{-3} for OC and EC, respectively, based on 72 m^3 of a typical sampling volume per sample. Both carbonaceous species were significantly higher than the LOD in all samples collected. The final carbonaceous mass on each filter was corrected with the field blank.

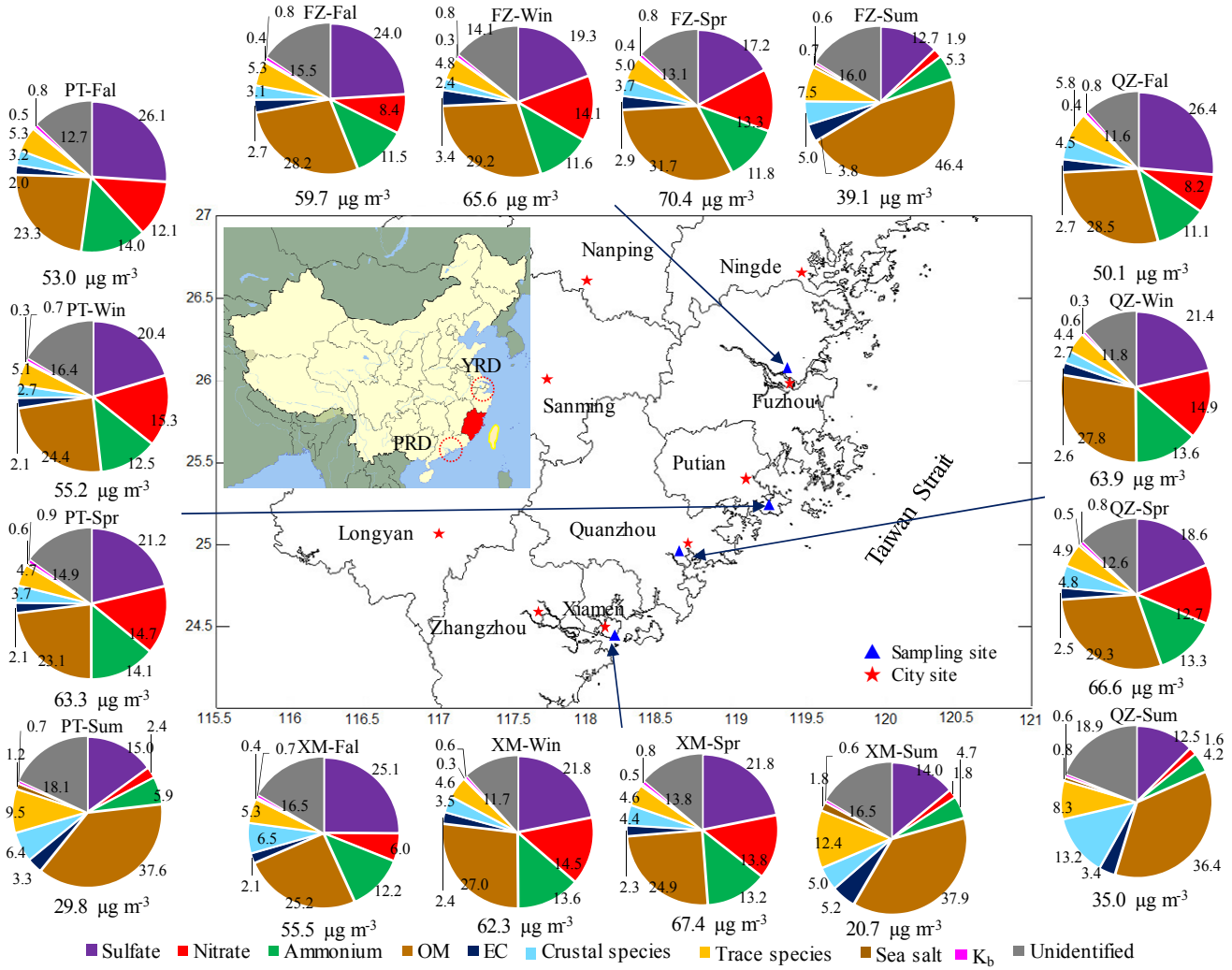

Fig. 1. Sampling sites and major chemical composition of $PM_{2.5}$ collected in urban Xiamen (XM), Quanzhou (QZ), Putian (PT) and Fuzhou (FZ). The numbers below pie charts represent the seasonal average of $PM_{2.5}$ mass concentration.

Water soluble ions including SO_4^{2-}, NO_3^-, NH_4^+, Cl^-, Na^+, Mg^{2+}, Ca^{2+}, and K^+ were analyzed using ion chromatography (PIC-10, Qingdao Puren Instruments Co., Ltd., China) with a suppressed conductivity detector. A universal cation column-MF (100 × 4.6 mm 7 μm, Alltech) and an anion column-MF (150 × 4.6 mm 7 μm, Allsep) were used to separate cations and anions. The mobile phase for cation and anion columns were 3.0 mM methanesulfonic acid and 0.85 mM $NaHCO_3$/0.9 mM Na_2CO_3, respectively. The determination coefficient (R^2) of the calibration curve for each ionic species was required to be higher than 0.99. Both field and laboratory blanks were routinely analyzed in order to correct the possible contamination due to the transportation and reagents. The spike recoveries were carried out by spiking with known amounts of standard ionic species to a blank filter punch, ranging from 86.7% (Cl^-) to 108% (NH_4^+). The field-blank based LOD were calculated as three times of the standard deviation of the field blanks and ranged from 0.03 μg m^{-3} (NO_3^-) to 0.77 μg m^{-3} (NH_4^+) based on 72 m^3 of sampling volume.

A total of 26 elements including F, Na, Mg, Al, Si, S, Cl, K, Ca, Ti, Zn, Fe, Pb, Mn, Cu, V, As, Br, Te, Ga, Cs, Ni, Cr, Cd, Co, and Se were determined by X-ray fluorescence (XRF-1800, Shimadzu, Japan). Standard filters with known amounts of the above elements (15–50 μg cm^{-2}) from Micromatter Company, Canada, were used to quantify the concentrations of these elements on polypropylene filters. The results were corrected by the field blanks.

Reconstruction of $PM_{2.5}$

As described in the introduction, carbonaceous species, secondary inorganic ions (SO_4^{2-}, NO_3^-, NH_4^+), and crustal elements such as Al, Si, Ca, and Fe are often the major components of $PM_{2.5}$ in Chinese urban areas. In this study, sulfate (SO_4^{2-}), nitrate (NO_3^-), ammonium (NH_4^+), organic matter (OM), EC, crustal species (Al_2O_3, SiO_2, CaO, and MgO and mineral part of Na_2O, K_2O, Fe_2O_3, MnO and TiO_2), trace species (F, Zn, Pb, Cu, V, As, Br, Te, Ga, Cs, Ni, Cr, Cd, Co and Se and non-mineral part of Fe, Mn and Ti), biomass burning-derived K^+ (K_b) and sea salt were included in the mass reconstruction of $PM_{2.5}$.

Because some chemical species were both measured

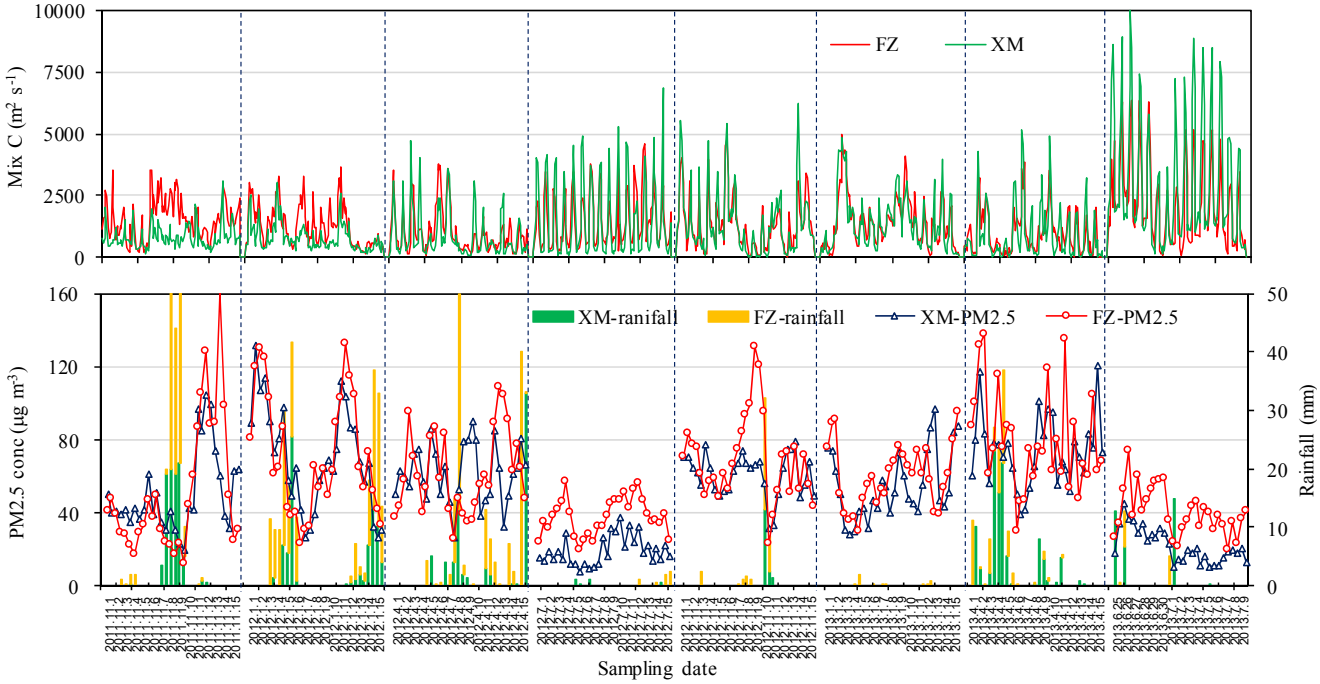

Fig. 2. Time series of hourly average vertical mixing coefficient and diurnal variations of $PM_{2.5}$ concentrations and rainfall during the eight sampling campaigns at XM and FZ sites.

using IC and XRF, it is necessary to compare the results to validate the data for $PM_{2.5}$ reconstruction. The ratio of SO_4^{2-} (using IC) to S (using XRF) is expected to be three, while the ratio of K^+ to K is expected to equal or be less than 1. A strong correlation was observed for SO_4^{2-} *vs.* total S (slope = 2.88, $R^2 = 0.91$, $p < 0.001$) and K^+ vs. total K (slope = 0.99, $R^2 = 0.80$, $p < 0.001$) (Fig. S1). Other species ratios such as Na^+/Na, Cl^-/Cl, Mg^{2+}/Mg, and Ca^{2+}/Ca (R^2 = 0.75) were also much less than 1. Thus, total Na, Ca, Mg, Cl and water soluble SO_4^{2-} and K^+ (used to calculate K_b) and Na^+ (only used to calculate sea salt) were used in the mass reconstruction of $PM_{2.5}$.

A factor of 1.6 in converting OC to OM was employed in this study in accordance with previous results (Turpin and Lim, 2001; Feng *et al.*, 2009; Xing *et al.*, 2013; Zhang *et al.*, 2013; Zhang *et al.*, 2015). The crustal species is estimated using a method provided by Zhao *et al.* (2010) and Yang *et al.* (2011):

$$\text{Crustal species} = 1.89 \times Al + 2.14 \times Si + 1.40 \times Ca + 1.67 \times Mg + 1.48 \times Al \quad (1)$$

The second Al coefficient (1.48) attempts to describe the contribution of other crustal elements (Na, K, Fe, Mn, and Ti), and their mineral oxides (Na_2O, K_2O, Fe_2O_3, MnO and TiO_2) are estimated from the Earth average crust composition (Taylor and McLennan, 1995; Yang *et al.*, 2011). The non-crustal fractions of K and Na were considered as biomass burning-derived K ($K_b = K^+ - 0.132 \times Al$) and sea-salt Na ($ssNa = Na^+ - 0.27 \times Al$), respectively. The residue mass, calculated as the mass difference between the measured $PM_{2.5}$ and the sum of the quantified species, was referred as unidentified. Therefore, $PM_{2.5}$ concentrations were reconstructed using the following equation:

$$PM_{2.5} = NH_4^+ + SO_4^{2-} + NO_3^- + OM + EC + \text{Crustal species} + \text{Trace species} + \text{Sea salt} + K_b + \text{Unidentified} \quad (2)$$

RESULTS AND DISCUSSION

$PM_{2.5}$ Concentrations

Summary statistics for mass concentrations of $PM_{2.5}$ and selected species are presented in Table 1. The annual average concentration of $PM_{2.5}$ at FZ site was slightly higher than those at XM, QZ and PT sites, but all exceed the current Ambient Air Quality Standards (GB 3905-2012) annual average of Grade II (35 μg m^{-3}) for urban $PM_{2.5}$ promulgated by China's Ministry of Environmental Protection and the annual average goal of 12 μg m^{-3} recommended by US EPA (EPA, 2013). On the other hand, the levels of $PM_{2.5}$ in this coastal urban zone were much lower than the values reported in other Chinese megacities such as Beijing, Tianjin, Shanghai, Chengdu, Jinan and Guangzhou in China and also higher than the previous levels measured in urban Fuzhou, Hong Kong and Seoul (Table 1). The average $PM_{2.5}$ concentrations at XM (54.99 μg m^{-3}), QZ (53.99 μg m^{-3}), PT (51.26 μg m^{-3}) and FZ (60.06 μg m^{-3}) observed in January 2013 were much lower than the reported values in the same sampling period at Beijing (158.5 μg m^{-3}), Xi'an (345.1 μg m^{-3}), Shanghai (90.7 μg m^{-3}) and Guangzhou (69.1 μg m^{-3}) reported in Huang *et al.* (2014). Although the fine particulate pollution is not as serious in Fujian as these other cities, health effects cannot be neglected based on the interim target-1 standard for annual mean $PM_{2.5}$ (35 μg m^{-3}) recommended by the WHO.

Table 1. Summary statistics of annual average concentrations of $PM_{2.5}$ and selected species at urban sites in different cities.

City	Sampling periods	$PM_{2.5}$	SO_4^{2-}	NO_3^-	NH_4^+	OC	EC	Al	Pb	Reference
Xiamen	2011–2013	51.45 ± 20.38	11.29 ± 5.52	5.50 ± 4.40	6.26 ± 4.02	8.65 ± 3.96	1.32 ± 0.22	0.21 ± 0.14	0.11 ± 0.10	This study
Quanzhou	2011–2013	53.91 ± 14.76	10.91 ± 4.96	5.67 ± 4.21	6.14 ± 4.00	10.05 ± 3.00	1.47 ± 0.27	0.26 ± 0.25	0.12 ± 0.11	This study
Putian	2011–2013	50.27 ± 14.38	10.72 ± 4.15	6.21 ± 3.68	6.24 ± 3.35	8.06 ± 2.04	1.15 ± 0.18	0.18 ± 0.12	0.11 ± 0.09	This study
Fuzhou	2011–2013	58.70 ± 14.77	11.02 ± 4.49	6.11 ± 3.90	6.23 ± 3.23	11.95 ± 2.85	1.83 ± 0.40	0.18 ± 0.13	0.12 ± 0.10	This study
Xiamen	2009–2010	72.12 ± 34.23	-	-	-	19.28 ± 9.48	3.30 ± 1.32	-		Zhang *et al.*, 2011
Fuzhou	2007–2008	44.33 ± 16.30	10.78 ± 4.85	4.40 ± 3.41	3.89 ± 3.04	8.50	2.17	0.47 ± 0.35	0.04 ± 0.02	Xu *et al.*, 2012
Beijing	1999–2000	88.6	10.15	7.26	4.28	18.21	6.67	1.37	0.26	He *et al.*, 2001
Beijing	2005–2006	118.5 ± 40.6	15.8 ± 10.34	10.1 ± 6.09	7.30 ± 4.17	24.5 ± 12.0	8.19 ± 5.96	0.79 ± 0.32	0.24 ± 0.12	Yang *et al.*, 2011
Beijing	2009–2010	135 ± 63	13.6 ± 12.4	11.3 ± 10.8	6.9 ± 7.1	16.9 ± 10.0	5.0 ± 4.4	1.8 ± 1.5	-	Zhang *et al.*, 2013
Beijing	2009–2010	123.45 ± 71.59	19.07 ± 16.36	20.47 ± 18.07	6.37 ± 3.91	18.15 ± 13.84	6.32 ± 2.93	0.97 ± 1.23	0.14 ± 0.11	Zhao *et al.*, 2013
Chongqing	2005–2006	129.0 ± 42.6	25.6 ± 9.03	5.46 ± 3.65	7.90 ± 3.78	30.13 ± 11.0	6.39 ± 2.56	0.80 ± 0.56	0.32 ± 0.12	Yang *et al.*, 2011
Tianjin	2009–2010	141.47 ± 78.03	24.97 ± 22.59	18.83 ± 15.77	7.64 ± 4.27	18.81 ± 12.90	6.86 ± 3.28	1.17 ± 1.32	0.22 ± 0.14	Zhao *et al.*, 2013
Shijiazhuang	2009–2010	191.19 ± 104.29	35.63 ± 23.00	30.38 ± 28.30	9.33 ± 4.47	26.52 ± 21.68	9.77 ± 4.81	1.41 ± 1.62	0.30 ± 0.22	Zhao *et al.*, 2013
Chengde	2009–2010	92.41 ± 54.62	13.00 ± 11.80	5.81 ± 7.31	4.06 ± 2.70	18.98 ± 16.07	7.41 ± 4.31	0.75 ± 0.69	0.11 ± 0.08	Zhao *et al.*, 2013
Jinan	2006–2007	148.71	30.92	10.58	13.99	22.19	4.10	0.86	0.30	Yang *et al.*, 2012
		97.59	18.43	5.49	7.97	20.20	4.33	0.34	0.25	Yang *et al.*, 2012
Shanghai	2005–2006	90.3 ± 54.9	-	-	-	14.7 ± 10.1	2.8 ± 1.3	-		Feng *et al.*, 2009
		95.5 ± 41.8	-	-	-	17.5 ± 9.8	3.0 ± 1.3	-		
Guangzhou	2008–2009	81.7 ± 25.6	5.6 ± 2.6	12.0 ± 5.1	4.7 ± 1.7	17.5 ± 7.6	4.1 ± 2.0	-	0.45 ± 0.21	Yang *et al.*, 2011
Chengdu	2011	119 ± 56	25.0 ± 14.1	10.7 ± 7.8	11.6 ± 7.3	17 ± 8	7 ± 4	0.56 ± 0.42	0.17 ± 0.09	Tao *et al.*, 2014
Nanjing	2011–2014	117.58 ± 77.97	-	-	-	13.75 ± 9.32	5.32 ± 3.11	-		Li *et al.*, 2015
Hong Kong	2000–2001	62.31 ± 18.57	9.44 ± 5.35	1.67 ± 1.70	3.16 ± 2.18	16.66 ± 7.63	20.18 ± 4.25	0.11 ± 0.11	0.07 ± 0.08	Louie *et al.*, 2005
Hong Kong	2002–2003	34.3 ± 14.1	9.3 ± 4.5	1.0 ± 0.7	2.5 ± 1.2	6.6 ± 3.1	1.9 ± 1.0		0.05–0.06	Hagler *et al.*, 2006
Seoul	2003–2006	43.50	8.11	7.06	5.27	10.52	3.53	0.26	0.05	Heo *et al.*, 2009

The seasonal variations of $PM_{2.5}$ are controlled by several meteorological factors such as ambient temperature (T), relative humidity (RH), atmospheric pressure (P), vertical mixing coefficient, rainfall, wind speed (WS) and direction (WD). In this region, cold seasons are generally characterized by northeast monsoon, occasional temperature inversions, high atmospheric pressure and low mixing coefficient which favor the long range transport of pollutants from the North and East China, and the accumulation of anthropogenic exhaust emissions. High temperature, high precipitation, low pressure, high mixing coefficient and southwest monsoon during the warm seasons would cause air pollutants to be diluted, dispersed, and washed out of the atmosphere. The concentrations of $PM_{2.5}$ at the four sites revealed a typical seasonality with higher values in fall, winter and spring, and lower values in summer (Figs. 1 and 2). It is clear that prevailing wind direction is south-southwest in summer and north-northeast in other seasons (Fig. S2(d)). The southwest winds blowing from the South China Sea will bring cleaner air masses and dilute the concentrations of $PM_{2.5}$ and related air pollutants. In contrast, the northern and northeastern winds along the mainland China's coastlines will bring more air pollutants and enhanced the concentrations of $PM_{2.5}$. In addition, higher mixing coefficient, wind speed, temperature and lower pressure in summer (Figs. 2(a), 2(c), 2(e) and 2(g)) helped $PM_{2.5}$ to disperse and resulted in lower $PM_{2.5}$ concentrations. Similar seasonal trends have also been observed for sulfur dioxide (SO_2), nitrogen dioxides (NO_2), nitric oxide (NO), PM_{10} and associated polycyclic aromatic hydrocarbons and organic acids in this area (Hsu *et al.*, 2010; Wu *et al.*, 2012; Xu *et al.*, 2012; Zhang *et al.*, 2012; Wu *et al.*, 2015). Significant associations were also found between $PM_{2.5}$ and some meteorological parameters such as wind speed, ambient temperature, pressure and mixing coefficient as well as its precursors such as SO_2 and NO_x at XM and FZ sites ($p < 0.001$) (Tables S1 and S2). Although these associations between $PM_{2.5}$ concentrations and rainfall (RF) and relative humidity (RH) were not significant during the whole sampling period, a drastic reduction in the concentration of $PM_{2.5}$ due to rain scavenging processes was seen in November 2011 and January 2012 (Fig. 2). The absence of statistical significance can be interpreted as ineffective wash-out of particulate matter by the light rain and/or a time lag between the reduction of $PM_{2.5}$ and the rain event. In addition, the mass concentrations of $PM_{2.5}$ at the four sites showed strong positive correlations ($r = 0.699–0.813$, $p < 0.001$) and very similar fluctuations and chemical composition (Fig. 1) during the same sampling period, which highlight the regional nature of the air pollution problem. These findings indicated that these sites shared a common flow of air or same airshed and/or had similar source categories (discussed later).

Major Chemical Components

Mass Closure

Based on the chemical analysis of these $PM_{2.5}$ samples, the major components included OM (30.2 ± 6.7%), sulfate (19.8 ± 5.1%), ammonium (10.6 ± 4.1%), and nitrate (9.7 ± 5.4%). The minor components included trace species (5.1 ± 2.1%), crustal species (4.7 ± 2.7%), EC (2.9 ± 0.9%), sea-salt (0.8 ± 0.6%) and biomass burning K (0.7 ± 0.1%). Unidentified components accounted for a significant fraction (15.5 ± 3.2%) of the $PM_{2.5}$ mass. Noticeably, the and OM ($r = 0.375–0.501$) at the significance of 0.001 (Table S1–S4). Huang *et al.* (2014) ascribed the high unidentified fraction (~35%) at an urban site in Xi'an to the elevated dust concentrations. Zhang *et al.* (2013) found the largest unidentified fraction in summer (42.5%) when secondary inorganic aerosol formation was favorable and smallest (15.9%) in spring when the dusts were prevalent in Beijing. In this study, no significant correlation was observed between unidentified and crustal species and sea-salt. Thus, the unidentified fraction may be attributed to the adsorbed water with the hygroscopic species such as sulfate, nitrate and ammonium during the transportation and condition (Xue *et al.*, 2014), and the selection of 1.6 as the conversion factor from OC to OM in this study (Turpin and Lim, 2001; Zhang *et al.*, 2013). A much higher conversion factor from OC to OM of up to 1.92 ± 0.39 was obtained in Chinese urban organic aerosols based on a mass balance method by Xing *et al.* (2013). Cao *et al.* (2013) also suggested a much higher factor of 3.2 from OC to OM if the carbonaceous aerosols were mainly formed from photochemical reactions.

Secondary Inorganic Ions

The contributions of sulfate, with an annual mean ranging from 10.72 ± 4.15 to 11.29 ± 5.52 μg m^{-3}, were significantly higher than nitrate (5.50 ± 4.40–5.67 ± 4.21 μg m^{-3}) and ammonium (6.14 ± 4.00–6.26 ± 4.02 μg m^{-3}) in accordance with the current Chinese energy structure with coal playing the main role (Wang *et al.*, 2013). The levels of the three inorganic species were significant lower than those observed at the Beijing, Tianjin, Jinan, and Chengdu urban sites and higher than those in Hong Kong and Fuzhou urban sites, especially for nitrate and ammonium (Table 1). The significant enhancement of nitrate and ammonium in Fuzhou urban area from 2007 to 2013 coincided with the growth of traffic pollutants followed by rapid urbanization observed in Beijing (He *et al.*, 2001; Yang *et al.*, 2011; Zhang *et al.*, 2013; Zhao *et al.*, 2013).

In average, the sum of sulfate, nitrate and ammonium (SNA) contributed 39.8–46.1% of the $PM_{2.5}$ mass at the four urban sites with lower values in summer (18.3–23.2%) and higher values in other seasons (43.2–52.2%) (Fig. 1). Fig. 3 shows the components driving the high $PM_{2.5}$ mass by binning the fractional contribution of each component to the total $PM_{2.5}$ mass in 10 μg m^{-3} unit intervals. The figure clearly shows that the elevated concentrations of $PM_{2.5}$ is characterized by an increasing SNA fraction, such as from 21% for $PM_{2.5}$ levels below 15 μg m^{-3} to 78% for $PM_{2.5}$ greater than 155 μg m^{-3}, demonstrating the importance of SNA formation in driving particulate pollution. Similar trends have also been observed for $PM_{2.5}$ collected during the episodes of 5–25 January 2013 at the urban sites of Beijing, Shanghai and Guangzhou (Huang *et al.*, 2014) and the periodic $PM_{2.5}$ episodes from 25 September to 13 November 2013 in Beijing (Guo *et al.*, 2014). Moreover, the fraction of nitrate to $PM_{2.5}$ along with the increase of

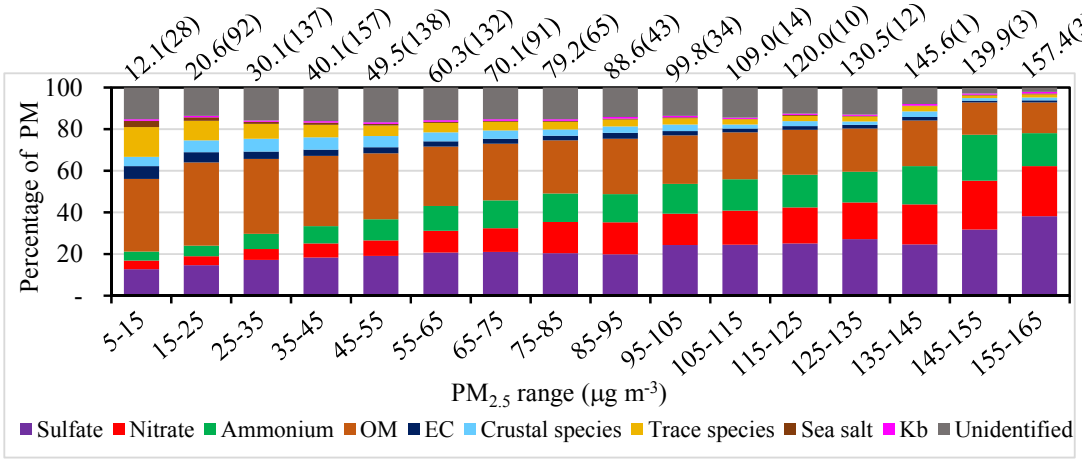

Fig. 3. Relative mass contributions for $PM_{2.5}$ in different ranges. The numbers above the bars represent the average $PM_{2.5}$ variability in the proportion for each component remained much stable during the same sampling season at the four sites (Fig. 1). This implied somewhat similar source categories, local or regional or both in this coastal zone. Moreover, the unidentified components showed well positive correlations with $PM_{2.5}$ mass (r = 0.611–0.671) as well as the three major inorganic ions (r = 0.355–0.654) concentration in μg m^{-3} and the number of samples in that range (inside of the parentheses).

$PM_{2.5}$ mass concentration increased at a faster rate (regression slope = 0.1366) than that of sulfate (regression slope = 0.1255) and ammonium (regression slope = 0.0948). This suggested that the emission control on nitrate precursors (mainly from motor vehicles) should be emphasized during the haze episodes in the area. However, due to the competition for bases (atmospheric ammonia) between nitrate and sulfate aerosol formation, the emission control on SO_2 and NO_x may not necessarily result in the decrease of nitrate aerosol due to more NO_x will react with NH_3 to form NH_4NO_3 (Lei and Wuebbles, 2013; Wang *et al.*, 2013).

In the Ammonia-Nitric Acid-Sulfuric Acid-Water System, the formation of nonvolatile $(NH_4)_2SO_4$ is preferred (Seinfeld and Pandis, 2006). Thus, the relationship between excess ammonium molar concentrations (defined as the ammonium minus the ammonium required to neutralize the available sulfate, i.e., $[NH_4^+]$-2$[SO_4^{2-}]$) and nitrate molar concentrations can be used to assess the formation of nitrate. Fig. 4 depicts the molar concentration comparison of excess ammonium vs. nitrate. When the ammonium is rich, excess ammonium will be available to react with nitrate to produce NH_4NO_3 (Seinfeld and Pandis, 2006; Pathak *et al.*, 2009). In our previous study, high emission fluxes of NH_3 and NO_x were found in the coastal urban areas due to high population and traffic densities while SO_2 showed a more scattered distribution in this coastal urban zone (Lu *et al.*, 2014). This condition is favorable for the in-situ formation of NH_4NO_3. For all the $PM_{2.5}$ samples, the Pearson's correlation coefficient between NH_4^+ and NO_3^- (r = 0.841–0.899, $p < 0.001$) were higher than that between NH_4^+ and SO_4^{2} (r = 0.787–0.847, $p < 0.001$) (Tables S1–S4) suggesting that NH_4NO_3 was present in substantial concentrations in this urban area. Moreover, the internal mixture of nitrate with sulfate could also reduce the thermodynamic dissociation constant Kn for NH_4NO_3, which would result in less loss of NH_4NO_3 through evaporation ($NH_4NO_{3(s)} \leftrightarrow NH_{3(g)} + HNO_{3(g)}$) (Zhao *et al.*, 2013).

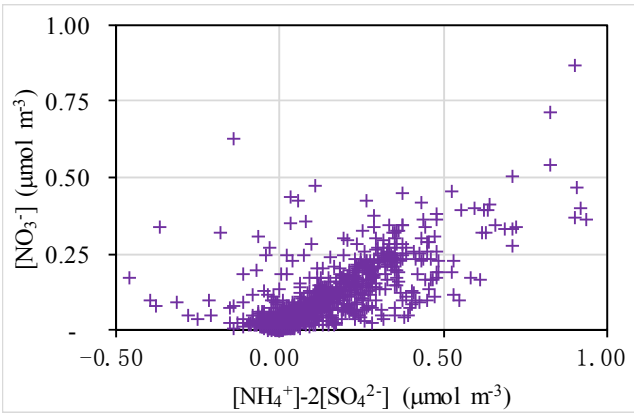

Fig. 4. Scatter plot of excess ammonium ionic charges ($[NH_4^+]$-2$[SO_4^{2-}]$) vs. nitrate ionic charges ($[NO_3^-]$).

At each sampling site, the ratios of NO_3^-/SO_4^{2-} had similar seasonal trends with the highest values in the winter (0.65–0.90) and spring (0.53–0.98), followed by those in fall (0.21–0.37) and summer (0.13–0.18) (Fig. S3(a)). Both NO_3^- and SO_4^{2-} as well as the ratio of NO_3^-/SO_4^{2-} were strongly anti-correlated with T ($P < 0.001$) indicating that NO_3^- was more sensitive to air temperature. Thus, the lowest NO_3^-/SO_4^{2-} ratios observed in summer were most likely due to the loss of NH_4NO_3 at high temperature (Zhao *et al.*, 2013). High NO_3^-/SO_4^{2-} in winter and spring suggested a less evaporation of NH_4NO_3 and a great fraction of particles resulted from vehicle exhausts. Besides, the influences of temperature, the transformation rate of sulfur dioxide (SO_2), nitrogen oxides (NO_x), and ammonia (NH_3) to sulfate, nitrate and ammonium could also influence the mass concentration and composition of SNA aerosols (Wang *et al.*, 2013). As shown in Fig. S4, the decrease of NOR in summer was more significant than that of SOR further indicating the influence of high temperature on nitrate loss.

In this study, the molar ratio of SO_4^{2-} to $SO_4^{2-} + SO_2$

defined as sulfur oxidation ratio (SOR) and the molar ratio of NO_3^- to NO_3^- + NO_x defined as nitrogen oxidation ratio (NOR) were used to evaluate the atmospheric transformation SO_2 to SO_4^{2-} and NO_x to NO_3^- at XM and FZ sites (Wang *et al.*, 2006; Fu *et al.*, 2008; Yang *et al.*, 2012; Squizzato *et al.*, 2013). Both of these ratios exhibited a similar seasonal trend, which was significantly low in summer and high in fall, winter, and spring (Fig. S3). These trends are similar to those observed in Shanghai (Wang *et al.*, 2006) and Venice (Squizzato *et al.*, 2013); but contrary to the results in Beijing and Jinan (Wang *et al.*, 2005; Yang *et al.*, 2012). The low SOR and NOR ratios in summer may be due to the unfavorable conditions, such as low concentrations of $PM_{2.5}$, SO_2, NO_x and O_3, for the homogeneous and heterogeneous gas-particle conversion of SO_2 and NO_x and less long-range transport processes carrying secondary sulfate and nitrate from surrounding air shed in the southwestern monsoon season (Fig. S4, Tables S1 and S2). Noticeably, much lower NOR values in fall were also observed due to high temperature and low relative humidity (Figs. S2, S4 and S9).

As shown in Tables S1 and S2, the strong positive correlations of SOR and NOR vs. O_3 and $PM_{2.5}$ likely indicated that the polluted atmosphere was favorable for the transformation of SO_2 and NO_x (Yang *et al.*, 2012). However, strong negative correlations between SOR and SO_2 were observed at both XM and FZ sites, which were completely different from the positive correlation between NOR and NO_x. On this basis it is apparent that nitrate was mainly from local formation, whereas sulfate was mainly transported from sources outside the coastal urban areas (Squizzato *et al.*, 2013). As for NOR, the significant low values found in summer could be more attributed to the loss of NH_4NO_3 at high temperature with average up to 30°C than to the low transformation rate of NO_x to NO_3^- (Zhao *et al.*, 2013). Moreover, the correlations between NOR and NH_4^+ and $PM_{2.5}$ ($r_{NOR\text{-}NH4+}$ = 0.722–0.806, $r_{NOR\text{-}PM2.5}$ = 0.749–0.790) were stronger than those of SOR with NH_4^+ and $PM_{2.5}$ ($r_{SOR\text{-}NH4+}$ = 0.480–0.612, $r_{SOR\text{-}PM2.5}$ = 0.487–0.605) suggesting that the formation of NO_3^- could occur through a gas-phase oxidation of NO_x in situ produced and enhanced due to the greater availability of NO_x and favorable meteorological conditions in the cold seasons (Squizzato *et al.*, 2013). But, the lack of HNO_3 data in this study would limit the further investigation about the formation mechanism of nitrate. Nevertheless, the positive feedback loop between the higher transformation of SO_2 and NO_x and the higher $PM_{2.5}$ was expected to result in an air pollution episode when there are stagnating meteorological conditions, such as low vertical mixing coefficients (Fig. 2).

Carbonaceous Species

As summarized in Table 1, the OC and EC annual mean in this study ranged from 8.06 ± 2.04 to 11.95 ± 2.85 μg m^{-3} and from 1.15 ± 0.18 to 1.83 ± 0.40 μg m^{-3}, respectively. Such levels were much lower than those observed at urban sites in the above listed megacities in China. Interestingly, the concentrations of EC at XM and FZ sites showed significant decreases compared those reported in previous studies in the same urban areas (Zhang *et al.*, 2011; Xu *et al.*, 2012). This improvement of air quality in terms of EC, which is usually recognized as a typical primary pollutant from vehicle exhausts in urban areas, may be more attributed to specific sampling site characteristics than to vehicle exhaust emission control. The urban sites for $PM_{2.5}$ measurement in Xiamen and Fuzhou in the previous studies (Zhang *et al.*, 2011; Xu *et al.*, 2012) are very close to busy traffic roadways, and may be subject to substantial influence of vehicular exhaust soot (EC), especially heavy duty diesel truck exhaust. Similarly, Louie *et al.* (2005) also measured very high EC levels (20.18 ± 4.25 μg m^{-3}) at a roadside site but much low levels at more secluded urban site (5.37 ± 1.40 μg m^{-3}) in Hong Kong.

On average, contrary to SNA mass contributions and NO_3^-/SO_4^{2-} mass ratios, carbonaceous aerosols and the ratios of OC to EC (OC/EC) showed weak seasonal variations (Fig. S2(b)). The highest relative contributions of carbonaceous aerosol to $PM_{2.5}$ mass are expected to be found in summer season due to the lowest $PM_{2.5}$ mass concentrations (Fig. 1). The OC/EC ratios in summer were close to or slightly higher than those in other seasons at each site except XM. At the XM site, the lowest OC/EC ratios were observed in summer and were similar to the trend reported in the same city in Zhang *et al.* (2011), probably due to its seashore position. As an island, Xiamen is affected by the influence of sea breeze and low OC/EC ratios are expected to be observed due to the decreased input of regional OC.

In this study, the contribution of secondary organic carbon (SOC) was estimated using an EC tracer method (Strader *et al.*, 1999; Cao *et al.*, 2007; Zhao *et al.*, 2013; Li *et al.*, 2015):

$$SOC = OC - EC \times (OC/EC)_{pri} \quad (3)$$

where $(OC/EC)_{pri}$ is the ratio for primary sources contributing to $PM_{2.5}$. Following the method in Feng *et al.* (2009) and Li *et al.* (2015), the values of $(OC/EC)_{pri}$ were simplified as the smallest observed ratio in the range of 2.80–5.21. These $(OC/EC)_{pri}$ ratios were comparable with 2.2–5.3 in Feng *et al.* (2009) but higher than 1.27–1.85 in Li *et al.* (2015). The difference of $(OC/EC)_{pri}$ in different studies may be related to analysis method of carbonaceous species. Watson *et al.* (2001) has pointed out that the OC/EC ratios measured by TOT method (in this study and Feng *et al.*, 2009) were comparatively higher than the ratios measured by TOR method (in Li *et al.*, 2015). Using this method SOC/OC ratios are shown in Fig. 5, and SOC accounted for 26–65% of the OC, suggesting that SOC is an important component of $PM_{2.5}$. The estimates of SOC to OC in this study were comparable with 25–46% in Nanjing (Li *et al.*, 2015), 27.0–33.2% in Shanghai (Feng *et al.*, 2009), 47.5–48.3% in Jinan (Yang *et al.*, 2012) and 43.4–58.8% in Xiamen suburban area (Zhang *et al.*, 2012). The higher fraction of SOC to OC observed in summer and fall may be related to the ambient conditions, such as the concentrations of O_3, $OH\cdot$ and $NO_3\cdot$ radicals as well as higher temperature and UV intensity (Seinfeld and Pandis, 2006). As presented in Fig. S5, much higher concentrations of O_3 were observed in spring and fall than in winter and summer. Higher concentrations of $NO_3\cdot$ radicals

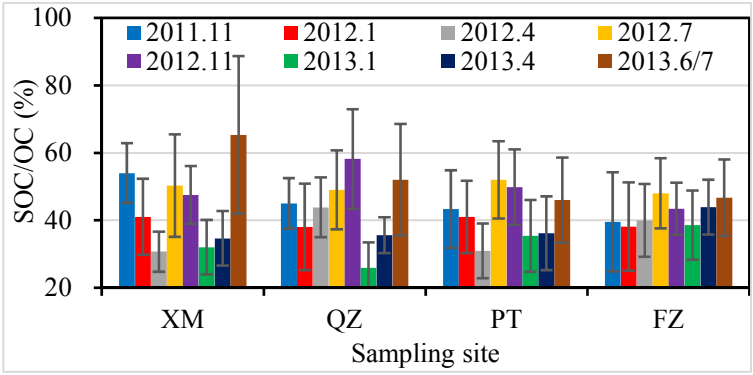

Fig. 5. Seasonal variations of SOC/OC ratio at the four sites.

are expected in spring and fall through the reaction of NO_2 with O_3 to form NO_3· radical (Vrekoussis *et al.*, 2007). However, higher ultraviolet intensity in summer can enhance the photolysis of O_3 and other compounds to produce more OH· radicals (Seinfeld and Pandis, 2006). These mechanisms may be used to explain the enhanced SOC/OC ratios in fall and summer as shown in Fig. 5. Similar seasonal trends of SOC/OC were also reported in Nanjing and Shanghai (Feng *et al.*, 2009; Li *et al.*, 2015). Nonetheless, the contribution of SOC to OC cannot be precisely determined because the formation of SOC is very complicated and can be affected by many ambient factors such as temperature, ultraviolet intensity, oxidant levels, particle characteristics and SOC precursors (Seinfeld and Pandis, 2006; Hsu *et al.*, 2010).

Inorganic Elements

As illustrated in Fig. 1, the crustal species in $PM_{2.5}$ was 1.0–4.6 μg m^{-3} and usually accounted for < 7% of $PM_{2.5}$ mass. Significant high loadings of crustal species were observed in November 2011 at the XM site (contributed 4.44 μg m^{-3} or accounted for 8.9% of $PM_{2.5}$) due to dust emission from residential construction and in July 2012 at the QZ site due to road excavation (contributed 5.89 μg m^{-3} or accounted for 15.3% of $PM_{2.5}$). The levels of crustal species are comparable to those measured in the urban areas of Hong Kong (2.4 ± 1.6 μg m^{-3}), Shenzhen (4.1 ± 2.3 μg m^{-3}), Guangzhou (6.6 ± 3.1 μg m^{-3}), and perhaps slightly lower than those in Beijing (5.5–8.4 μg m^{-3}) and Chongqing (7.6–9.9 μg m^{-3}) (Hagler *et al.*, 2006; Yang *et al.*, 2011). Similarly, Al, as a marker for crustal species, also showed much lower levels when compared to those reported in Chinese megacities (Table 1). Furthermore, the ratios of Si to Al (Si/Al) showed lower values in summer (1.8–2.1) than in other seasons (2.2–2.8). Lower Si/Al ratios have been observed in soil (1.46–1.89) than those in road dusts (2.13–2.24) in this coastal urban area (Zheng *et al.*, 2013). In Hong Kong, lower Si/Al ratios in soils (1.25–1.55) than those in road dusts (2.56) and cements (3.93) were also observed (Ho *et al.*, 2003). Based on the seasonal variations of Si/Al, road dusts may have less influence on $PM_{2.5}$ in summer than in other seasons. In general, the relative contributions of crustal species to $PM_{2.5}$ showed high values in summer due to the lower $PM_{2.5}$ mass. The trend of relative contribution is clearly shown in Fig. 3, suggesting that the frequent road watering widely used in Xiamen and other cities in this coastal urban area for adding humidity and reducing urban road dust resuspension will not help to reduce fine particulate levels efficiently.

The concentrations of trace species were slightly higher than those of crustal species with values in the range of 2.6–3.5 μg m^{-3}. The values are higher than those in Hong Kong (1.0 ± 0.3 μg m^{-3}) and Shenzhen (1.6 ± 0.9 μg m^{-3}), and comparable with 2.5 ± 1.3 μg m^{-3} in Guangzhou, 1.4–2.3 μg m^{-3} in Beijing and 2.4–4.0 μg m^{-3} in Chongqing (Hagler *et al.*, 2006; Yang *et al.*, 2011). Similar to crustal species, higher relative contributions of trace species to $PM_{2.5}$ were observed in summer than in other seasons (Fig. 1). Pb and K_b, mainly emitted from fuel combustion/industrial activities and biomass burning, were at trace levels in samples and showed similar seasonal trends with lower values in summer and higher in other seasons (Table 1). The annual average concentrations of Pb were 0.11–0.12 μg m^{-3} at all four urban sites, and were close to the mean wintertime concentrations (0.095 μg m^{-3}) in PM_{10} collected from Kinmen Island (an offshore island close to Xiamen Island) (Hsu *et al.*, 2010) but lower than those reported levels in other Chinese megacities listed in Table 1. On average, the calculated K_b levels were 0.37–0.45 μg m^{-3} and accounted for 81–88% of measured K^+. At all sampling sites, Pb and K_b were positively correlated with Fe, Mn, Zn, and EC ($r = 0.204–0.641$, $p < 0.01$) but not with Al and Si. The stronger correlation among Pb, Zn, Mn, Fe and K_b suggested their common sources such as vehicular exhausts, metal processing and biomass burning and/or similar atmospheric fate under the common synoptic conditions. Although our study location was close to the coast line, sea salt comprised only 0.3–1.8% of $PM_{2.5}$ mass, which was similar to the observations made in USA (Malm *et al.*, 2004), probably due to the size distribution of Na^+ which was dominanted by the coarse mode (> 2.5 μm) (Bian *et al.*, 2014).

Reconstructed Aerosol Light Extinction Coefficient

In addition the adverse health effects of $PM_{2.5}$, it can also result in atmospheric visibility deterioration through light extinction (IMPROVE, 2010). In this study, the visibility is anti-correlated with the mass concentration of $PM_{2.5}$ and its major components and meteorological parameters ($p < 0.001$) at both XM and FZ sites (Table S1 and S2), consistent with previous studies (Yang *et al.*, 2007; Huang *et al.*, 2009; Cao

et al., 2012). For the relation between visibility and $PM_{2.5}$ mass concentration, we find the logarithmic function that best fits the data at both XM and FZ sites (Fig. 6), and find different functional fits from those established in Jinan by Yang *et al.* (2007) and in Xi'an by Cao *et al.* (2012). Furthermore, the coefficient of determination (R^2) increased when the samples collected in rainy days were removed, most markedly at the FZ site. The results clearly showed that $PM_{2.5}$ levels need to be reduced more to enhance visibility from 5 to 10 km than from 10 to 15 km.

We also used the revised IMPROVE algorithm to estimate aerosol light extinction coefficients (b_{ext}) (Pitchford *et al.*, 2007). The algorithm included contributions from ammonium sulfate (AS), ammonium nitrate (AN), organic matter (OM), elemental carbon (EC), soil, coarse mass (PM_{10}–$PM_{2.5}$), NO_2 and site-specific Rayleigh scattering of clear air:

$$b_{ext} \approx 2.2 \times f_S(RH) \times [\text{small AS}] + 4.8 \times f_L(RH) \times [\text{large AS}] + 2.4 \times f_S(RH) \times [\text{small AN}] + 5.1 \times f_L(RH) \times [\text{large AN}] + 2.8 \times [\text{small OM}] + 6.1 \times [\text{large OM}] + 10 \times [\text{EC}] + 1 \times [\text{Soil dust}] + 1.7 \times f_{SS}(RH) \times [\text{Sea salt}] + 0.6 \times [\text{Coarse mass}] + 0.33 \times [NO_2(\text{ppb})] + \text{site-specific Rayleigh Scattering} \quad (4)$$

where $f_S(RH)$ and $f_L(RH)$ are scattering enhancement factors for small and large AS/AN, $f_{SS}(RH)$ refers to sea salt. The site-specific Rayleigh scattering coefficient was assumed to be a constant value of 12 Mm^{-1} near sea level. In the urban areas, PM_{10} was around two times of $PM_{2.5}$ (1.81 ± 0.18–2.30 ± 0.42) during the sampling period based on the data from Fujian Environmental Protection Bureau, which was close to 1.91 in Shanghai (Huang *et al.*, 2009). The details of the small/large split component approach and parameters can be obtained from Pitchford *et al.* (2007). Predicted visibilities in km express as reconstructed deciview were calculated from Koschmeider equation (Seinfeld and Pandis, 2006):

$$\text{Predicted Visibility} = 3.912/b_{ext} \quad (5)$$

The predicted visibility using revised IMPROVE method correlated well ($P < 0.001$) with the measured visibility with a regression slope of 0.80–1.10 (Fig. S6), indicating that $PM_{2.5}$ and related air pollutants can be used to predict visibility. Noticeably, at the XM site there appeared to be more large deviations of predicted *vs* observed visibility above the 1:1 line, whereas at the FZ site the deviations were greater below this line. More information about the mixing states (internal and external) and more locally-derived dry light scattering and absorption coefficients and f(RH) might improve the agreement (Pitchford *et al.*, 2007; Cao *et al.*, 2012). As shown in Fig. S7, the lowest values of b_{ext} were found in summer and the highest values were found in winter or spring, with an annual average of 339 ± 265 Mm^{-1} and 436 ± 310 Mm^{-1} at XM and FZ, respectively. The reconstructed b_{ext} at XM and FZ sites were much lower than 912 ± 882 Mm^{-1} in Xi'an (Cao *et al.*, 2012) and 704 Mm^{-1} in Seoul (Kim *et al.*, 2006) and slight higher than 292 Mm^{-1} in Jinan (Yang *et al.*, 2007) and 214 Mm^{-1} in peri-urban of Xiamen (Zhang *et al.*, 2012). Moreover, the calculated contributions of the major species to b_{ext} showed different seasonal patterns. Ammonium sulfate was not always the largest contributor (except in summer) accounting 15–43% of b_{ext}, different from previous studies in Xi'an (Cao *et al.*, 2012) and Jinan (Yang *et al.*, 2007). Another three important contributors were AN (2–31%), OM (13–47%) and coarse mass (11–21%). EC was the minor contributor due to its much low contribution (3–10%). These results suggest that the visibility is strongly connected to fine particulate matter and emission reduction of SNA and OM could help achieving a better visibility.

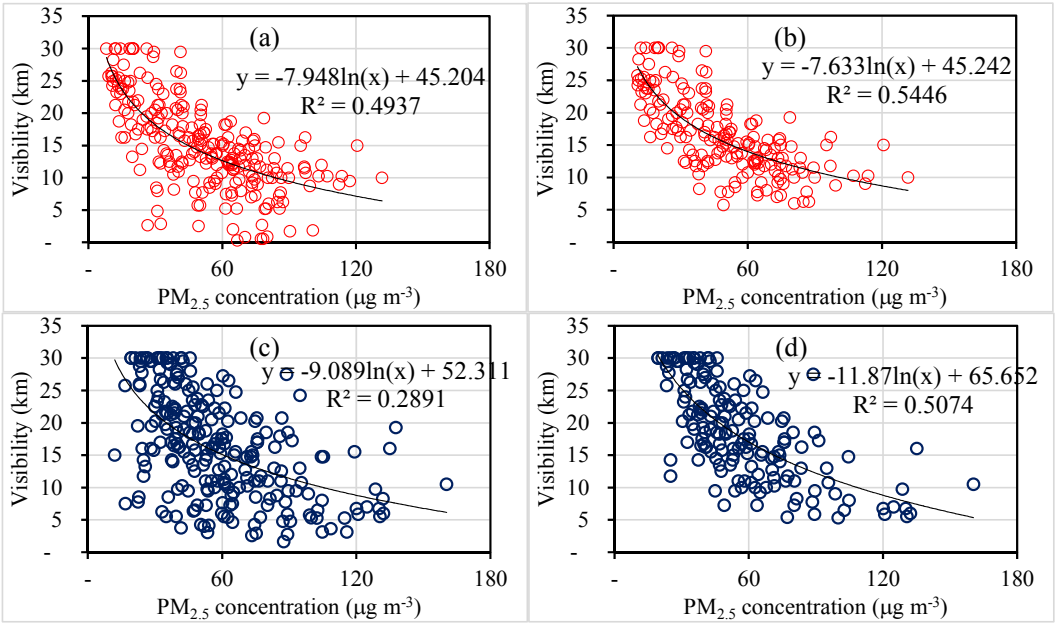

Fig. 6. Scatter plot of $PM_{2.5}$ mass concentration vs. visibility at XM (a-total samples; b-samples without precipitation) and FZ (c-total samples; d-samples without precipitation) sites.

Diurnal Variations

It can be seen from Fig. 2 that the time series of $PM_{2.5}$ coincided well with rainfall. In most cases, rain wash-out could remove $PM_{2.5}$ to a great extent. Higher pressure and lower vertical mixing coefficient, were another two important drivers for air pollutants accumulation, especially during the sampling periods without significant rainfall (Figs. S2, S8 and S9). For example, the low levels of $PM_{2.5}$ measured between 5–7 July 2012 could be attributed to the increase of mixing coefficient (or wind speed) and air pressure. However, in 2013 summer, the significant decrease of $PM_{2.5}$ from June 30 to July 1 were more related to wind direction which shifted from the southwest to the north and the northeast due to the effects of typhoon Rumbia moving northwestward to the South China (http://en.wikipedia.org/wiki/Tropical_Storm_Rumbia_(2013)).

Notice that after a rain event $PM_{2.5}$ mass concentration could recover and approach another peak rapidly in 1–3 days which showed a peak-valley cycle (Fig. 2). Rain events appeared to be the most important meteorological factor in driving the periodic $PM_{2.5}$ cycle, which was different from that in Beijing where the wind direction and speed controlled the periodic $PM_{2.5}$ cycle (Guo *et al.*, 2014). This peak-valley cycle also indicated the existence of strong emission sources which contribute to the air pollution episodes in appropriate meteorological conditions. As shown in Tables S1–S2, the strong positive correlation relationships between $PM_{2.5}$ major components and precursors (SO_2 and NO_x) as well as oxidation ratios (SOR and NOR) and O_3, indicating an important role of photochemical activity in the formation of particle phase SNA and OM. The unfavorable dispersion conditions drive the positive feedback loop between precursors and secondary aerosols as illustrated before. Once the meteorological drivers become weak and even negative (e.g., rain wash out), clear air is expected.

Since the meteorological parameters in summer presented in Fig. S8 showed zigzag day-night variations, similar regular trends were also expected for $PM_{2.5}$ and associated air pollutants. In summer, $PM_{2.5}$ mass concentrations were slight higher in daytime than at nighttime (Fig. S9). These patterns might be greatly influenced by OM and sulfate due to their high contributions (48.9–59.1%) to $PM_{2.5}$ as illustrated in Fig. 1. It can be seen from Fig. S9, the day-night trends of SO_2 and O_3 were similar to those of sulfate and OM. However, NO_2 and nitrate concentrations showed clear diurnal variations with higher values during nighttime. This might have been due to the photolysis of NO_2 by UV light which resulted in higher O_3 during the day. Owing to the combined effect of higher NO_2 and RH, and lower temperatures during the nighttime (Figs. S8 and S9), more nitrate were produced. In spite of this, the contribution of nitrate to $PM_{2.5}$ (less than 2.5% on average in summer) is too low to offset the contribution of sulfate and OM. Noticeably, the stronger sea breeze from south-southeast and higher mixing coefficient during the daytime (Fig. S8) didn't dilute the air pollutants to a great extent and disrupt the day-night variation patterns due to the strong daytime secondary transformation (except for nitrate formation). In other seasons, the frequent rain scavenging as well as no regular day-night difference for mixing coefficient could interrupt and overwhelm the regular day-night photochemical differences.

CONCLUSIONS

Intensive $PM_{2.5}$ sampling was carried out and analyzed for its chemical composition and temporal variations at four urban sites in the southeast coastal area of China. The annual average levels of $PM_{2.5}$ obtained in this study obviously exceeded the annual level of Grade II (35 μg m^{-3}) given in China's latest Ambient Air Quality Standards (GB 3095-2012), but at the same time are lower than those reported in other Chinese megacities. At the four sites, organic matter was always the single largest component followed by sulfate, ammonium and nitrate, and their variability remained stable during the same sampling season. The significant predominance of sulfate over nitrate (around two-fold) indicated the importance of promoting clean coal combustion for control of air pollution in this area. Sulfate, nitrate and ammonium were the most important drivers of $PM_{2.5}$ episodes. The increasing contribution of nitrate to $PM_{2.5}$ compared to sulfate during haze episodes further emphasized the importance of local vehicle exhausts in the urban area. The seasonal variations of $PM_{2.5}$ and its major components at the four sites were similar with lower levels in summer and higher in other seasons which were associated with the summer southwest monsoon and other season's northeast monsoon.

Rainfall scavenging was the most critical parameter in driving the periodic $PM_{2.5}$ cycle, which was different from that in Beijing where the wind direction and speed played the major role. Under appropriate meteorological conditions, the formation of positive feedback loop between enhanced primary pollutants and transformation rates and $PM_{2.5}$ played the most important role in the formation of pollution episode in this coastal urban zone. Regular diurnal variations were only observed in summer when there existed regular variations for meteorological parameters but with no significant rainfall and external input. Although the atmospheric dispersion conditions were better during the daytime than nighttime in summer, the daytime predominant $PM_{2.5}$ was observed due to the more production of sulfate and organic aerosols through secondary photochemical reactions. Measured visibility variations correlated well with the predicted visibility based on the revised IMPROVE method, reflecting that visibility is an indicator of urban air quality. Up to 80% light extinction coefficient was contributed from ammonium sulfate, ammonium nitrate and organic matter. Considering the similarities in the chemical composition and the synchronous variations of $PM_{2.5}$ at the four sites, this coastal urban zone would be an appropriate place to investigate the regional-scale $PM_{2.5}$ pollution extending from YRD to PRD along the coastal lines of Eastern China.

ACKNOWLEDGEMENTS

This work is supported by the National Natural Science Foundation of China (41471390, 41171365), and also by the China Ministry of Environmental Protection's Special Funds for Scientific Research on Public Welfare (201009004)

and the Program for Changjiang Scholars and Innovative Research Team in University (PCSIRT) (IRT0941).

SUPPLEMENTARY MATERIALS

Supplementary data associated with this article can be found in the online version at http://www.aaqr.org.

REFERENCES

Bian, Q., Huang, X.H.H. and Yu, J.Z. (2014). One-Year Observations of Size Distribution Characteristics of Major Aerosol Constituents at a Coastal Receptor Site in Hong Kong - Part 1: Inorganic Ions and Oxalate. *Atmos. Chem. Phys*. 14: 9013–9027.

Birch, M.E. and Cary, R.A. (1996). Elemental Carbon-Based Method for Occupational Monitoring of Particulate diesel Exhaust: Methodology and Exposure Issues. *Analyst* 121: 1181–1190.

Cao, J.J., Lee, S.C., Chow, J.C., Watson, J.G., Ho, K.F. and Zhang, R.J. (2007). Spatial and Seasonal Distribution of Carbonaceous Aerosols over China, 2007. *J. Geophys. Res*. 112: D22S11.

Cao, J.J., Wang, Q.Y., Chow, J.C., Watson, J.G., Tie, X.X., Shen, Z.X., Wang, P. and An, Z.S. (2012). Impacts of Aerosol Compositions on Visibility Impairment in Xi'an, China. *Atmos. Environ.* 59: 559–566.

Cao, J.J., Zhu, C.S., Tie, X.X., Geng, F.H., Hu, H.M., Ho, S.S.H., Wang, G.H., Han, Y.M. and Ho, K.F. (2013). Characterisstics and Source of Carbonaceous Aerosols from Shanghai, China. *Atmos. Chem. Phys*. 13: 803–817.

Feng, Y., Chen, Y., Guo, H., Zhi, G., Xiong, S., Li, J., Sheng, G. and Fu, J. (2009). Characteristics of Organic and Elemental carbon in $PM_{2.5}$ Samples in Shanghai, China. *Atmos. Res.* 92: 434–442.

Fu, Q., Zhuang, G., Wang, J., Xu, C., Huang, K., Li, J., Hou, B., Lu, T. and Street, D.G. (2008). Mechanism of Formation of the Heaviest Pollution Episode ever Recorded in the Yangtze River Delta, China. *Atmos. Environ*. 42: 2023–2036.

Guo, S., Hu, M., Zamora, M.L., Peng, J., Shang, D., Zheng, J., Du, Z., Wu, Z., Shao, M., Zeng, L., Molina, M.J. and Zhang, R. (2014). Elucidating Severe Urban Haze Formation in China. *PNAS* 111: 17373–17378.

Hagler, G.S.W, Bergin, M.H., Salmon, L.G., Yu, J.Z., Wan, E.C.H., Zheng, M., Zeng, L.M., Kiang, C.S., Zhang, Y.H., Lau, A.K.H. and Schauer, J.J. (2006). Source Areas and Chemical Composition of Fine Particulate Matter in the Pearl River Delta Region of China. *Atmos. Environ.* 40: 3802–3815.

He, K., Yang, F., Ma, Y., Zhang, Q., Yao, X., Chan, C.K., Cadle, S., Chan, T. and Mulawa, P. (2001). The Characteristics of $PM_{2.5}$ in Beijing, China. *Atmos. Environ*. 35: 4959–4970.

Henriksson, S.V., Laaksonen, A., Kerminen, V.M., Räisänen, P., Järvinen, H., Sundström, A.M. and Leeuw, G. de. (2011). Spatial Distributions and Seasonal Cycles of Aerosols in India and China Seen in global Climate-Aerosol Model. *Atmos. Chem. Phys.* 11: 7975–7990.

Heo, J.B., Hopke, P.K. and Yi, S.M. (2009). Source Apportionment of $PM_{2.5}$ in Seoul, Korea. *Atmos. Chem. Phys*. 9: 4957–4971.

Ho, K.F., Lee, S.C., Chow, J.C. and Watson, J.G. (2003). Characterization of PM_{10} and $PM_{2.5}$ Source Profiles for Fugitive Dust in Hong Kong. *Atmos. Environ.* 37: 1023–1032.

Hsu, S.C., Liu, S.C., Tsai, F., Engling, G., Lin, I.I., Chou, C.K.C., Kao, S.J., Lung, S.C.C., Chan, C.Y., Lin, S.C., Huang, J.C., Chi, K.H., Chen, W.N., Lin, F.J., Huang, C.H., Kuo, C.L., Wu, T.C. and Huang, Y.T. (2010). High Wintertime Particulate Matter Pollution over an Offshore Island (Kinmen) off Southeastern China: An Overview. *J. Geophys. Res.* 115: D17309, doi: 10.1029/2009JD013641.

Huang, R.J., Zhang, Y., Bozzetti, C., Ho, K.F., Cao, J.J., Han, Y., Daellenbach, K.R., Slowik, J.G., Platt, S.M., Canonaco, F., Zotter, P., Wolf, R., Pieber, S.M., Bruns, E.A., Crippa, M., Ciarelli, G., Piazzalunga, A., Schwikowski, M., Abbaszade, G., Schnelle-Kreis, J., Zimmermann, R., Am, Z., Szidat, S., Baltensperger, U., Haddad, I.E. and Prévôvt, A.S. (2014). High Secondary Aerosol Contribution to Particulate Pollution during Haze Events in China. *Natural* 514: 218–222

Huang, W., Tan, J., Kan, H., Zhao, N., Song, W., Song, G., Chen, G., Jiang, L., Jiang, C., Chen, R. and Chen, B. (2009). Visibility, Air Quality and Daily Mortality in Shanghai, China. *Sci. Total Environ*. 407: 3295–3300.

Huang, X.H.H., Bian, Q., Ng, W.M., Louie, P.K.K. and Yu, J.Z. (2014). Characterization of $PM_{2.5}$ Major Components and Source Investigation in Suburban Hong Kong: A One Year Monitoring Study. *Aerosol Air Qual. Res.* 14: 237–250.

IMPROVE (2010). Spatial and Seasonal Patterns and Temporal Variability of Haze and its Constituents in the United States. Report IV.

Kim, Y.J., Kim, K.W., Kim, S.D., Lee, B.K. and Han, J.S. (2006). Fine Particulate Matter Characteristics and its Impact on Visibility Impairment at Two Urban Sites in Korea: Seoul and Incheon. *Atmos. Environ*. 40: 593–605.

Lei, H., Wuebbles, D.J. (2013). Chemical Competition in Nitrate and Sulfate Formations and Its Effect on Air Quality. *Atmos. Environ*. 80: 472–477.

Li, B., Zhang, J., Zhao, Y., Yuan, S., Zhao, Q., Shen, G. and Wu, H. (2015). Seasonal Variation of Urban Carbonaceous Aerosols in a Typical City Nanjing in Yangtz River Delta, China. *Atmos. Environ*. 106: 223–231.

Li, T.C., Chen, W.H., Yuan, C.S., Wu, S.P. and Wang, X.H. (2013a). Physicochemical Characteristics and Source Apportionment of Atmospheric Aerosol Particles in Kinmen-Xiamen Airshed. *Aerosol Air Qual. Res.* 13: 308–323.

Li, T.C., Wu, C.Y., Chen, W.H., Yuan, C.S., Wu, S.P., Wang, X.H. and Du, K. (2013b). Diurnal Variation and Chemical Characteristics of Atmospheric Aerosol Particles and Their Source Fingerprints at Xiamen Bay. *Aerosol Air Qual. Res.* 13: 596–607.

Louie, P.K.K., Chow, J.C., Chen, L.W.A., Watson, J.G., Leung, G.L., Sin, D.W.M. (2005). $PM_{2.5}$ Chemical Composition in Hong Kong: Urban and Regional

Variations. *Sci. Total Environ*. 338: 267–281.

Lu, S.W, Hu, Q.H., Wu, S.P. and Chen, X.Q. (2014). Establishment of Air Pollutants Emission Inventory in the West Coast of Taiwan Straits. *Acta Sci. Circumst.* 34: 3624–3634 (in Chinese with English Abstract).

Malm, W.C., Schichtel, B.A., Pitchford, M.L, Ashbaugh, L.L and Eldred, R.A. (2004). Spatial and Monthly Trends in Speciated Fine Particle Concentration in the United States. *J. Geophys. Res.* 109: D03306, doi: 10.1029/2003 JD003739.

Pathak, R.K., Wu, W.S. and Wang, T. (2009). Summertime $PM_{2.5}$ Ionic Species in Four Major Cities of China: Nitrate Formation in an Ammonia-deficient Atmosphere. *Atmos. Chem. Phys.* 9: 1711–1722.

Pitchford, M., Mal, W., Schichtel, B., Kumar, N., Lowenthal, D. and Hand, J. (2007). Revised Algorithm for Estimating light Extinction from IMPROVE Particle Speciation Data. *J. Air Waste Manage. Assoc.* 57: 1326–1336.

Seinfeld, J.H. and Pandis, S.N. (2006). *Atmospheric Chemistry and Physics: from Air Pollution to Climate Change*, 2nd Edition, John Wiley and Sons, New Jersey.

Song, Y., Zhang, Y., Xie, S., Zeng, L., Zheng, M., Salmon, L.G., Shao, M. and Slanina, S. (2006). Source Apportionment of $PM_{2.5}$ in Beijing by Positive Matrix Factorization. *Atmos. Environ.* 40: 1526–1537.

Squizzato, S., Masiol, M., Brunelli, A., Pistollato, S., Tarabotti, E., Rampazzo, G. and Pavoni, B. (2013). Factors Determining the Formation of Secondary Inorganic Aerosol: A Case Study in the Po Valley (Italy). *Atmos. Chem. Phys.* 13: 1927–1939.

Strader, R., Lurmann, F. and Pandis, S.N. (1999). Evaluation of Secondary Organic Aerosol Formation in Winter. *Atmos. Environ.* 33: 4849–4863.

Sun, Y., Zhuang, G., Tang, A., Wang, Y. and An, Z. (2006). Chemical Characteristics of $PM_{2.5}$ and PM_{10} in Haze-Fog Episodes in Beijing. *Environ. Sci. Technol*. 40: 3148–3155.

Tao, J., Gao, J., Zhang, L., Zhang, R., Che, H., Zhang, Z., Lin, Z., Jing, J., Cao, J. and Hsu, S.C. (2014). $PM_{2.5}$ Pollution in a Megacity of Southwest China: Source Apportionment and Implication. *Atmos. Chem. Phys.* 14: 8679–8699.

Taylor, S.R. and McLennan, S.M. (1995). The Geochemical Evolution of the Continental-Crust. *Rev. Geophys.* 33: 241–265.

Turpin, B. J. and Lim, H.J. (2001). Species Contributions to $PM_{2.5}$ mass Concentrations: Revisiting Common Assumptions for Estimating Organic Mass. *Aerosol Sci. Technol.* 35: 602–610.

Vrekoussis, M., Mihalopoulos, N., Gerasopolos, E., Kanakidou, M., Crutzen, P.J. and Lelieveld, J. (2007). Two-Years of No.3 Radical Obzervations in the Boundary Layer over the Eastern Mediterranean. *Atmos. Chem. Phys*. 7: 315–327.

Wang, Y., Zhuang, G., Zhang, X., Huang, K., Xu, C., Tang, A., Chen, J. and An, Z. (2006). The Ion Chemistry, Seasonal Cycle, and Sources of $PM_{2.5}$ and TSP Aerosol in Shanghai. *Atmos. Environ*. 40: 2935–2952.

Wang, Y., Zhang Q.Q., He, K., Zhang, Q. and Chai, L. (2013). Sulfate-Nitrate-Ammonium Aerosols over China: Response to 2000–2015 Emission Changes of Sulfur Dioxide, Nitrogen Oxides, and Ammonia. *Atmos. Chem. Phys*. 13: 2635–2652.

Watson, J.G., Chow, J.C. and Houck, J.E. (2001). $PM_{2.5}$ Chemical Source Profiles for Vehicle Exhaust, Vegetative Burning, Geological Material, and Coal Burning in Northwestern Colorado during 1995. *Chemosphere* 43: 1141–1151.

Wu, S.P., Qian, R.R., Lee, T.C., Wang, X.H., Hong, H.S. and Yuan, C.S. (2012). Seasonal Variation for the Ratio of BaP to BeP at Different Sites in Great Xiamen Bay. *J. Environ. Monit*. 14: 1220–1229.

Wu, S.P., Schwab, J., Liu, B.L., Li, T.C. and Yuan, C.S. (2015). Seasonal Variations and Source Identification of Selected Organic Acids Associated with PM_{10} in the Coastal Area of Southeastern China. *Atmos. Res*. 155: 37–51.

Xing, L., Fu, T.M., Cao, J.J, Lee, S.C., Wang, G.H., Ho, K.F., Cheng, M.C., You, C.F. and Wang, T.J. (2013). Seasonal and Spatial Variability of the OM/OC Mass Ratios and High Regional Correlation between Oxalic Acid and Zinc in Chinese Urban Organic Aerosols. *Atmos. Chem. Phys.* 13: 4307–4318.

Xu, L., Chen, X., Chen, J., Zhang, F., He, C., Zhao, J. and Yin, L. (2012). Seasonal Variations and Chemical Composition of $PM_{2.5}$ Aerosol in the Urban Area of Fuzhou, China. *Atmos. Res.* 104–105: 264–272.

Xue, J., Grith, S.M., Yu, X., Lau, A. K.H. and Yu, J.Z. (2014). Effect of Nitrate and Sulfate Relative Abundance in $PM_{2.5}$ on Liquid Water Content Explored through Half-Hourly Observations of Inorganic Soluble Aerosols at a Polluted Receptor Site. *Atmos. Environ*. 99: 24–31.

Yang, F., Tan, J., Zhao, Q., Du, Z., He, K., Ma, Y., Duan, F., Chen, G. and Zhao, Q. (2011). Characteristics of $PM_{2.5}$ Speciation in Representative Megacities and across China. *Atmos. Chem. Phys. Discuss.* 11: 1025–1051.

Yang, L., Zhou, X., Wang, Z., Zhou, Y., Cheng, S., Xu, P., Gao, X., Nie, W., Wang, X. and Wang, W. (2012). Airborne Fine Particulate Pollution in Jinan, China: Concentrations, Chemical Compositions and Influence on Visibility Impairment *Atmos. Environ*. 55: 506–514.

Yang, L.X., Wang, D.S., Cheng, S.H., Wang, Z., Zhou, Y., Zhou, X.H. and Wang, W.X. (2007). Influence of Meteorological Conditions and Particulate Matter on Visual Range Impairment in Jinan, China. *Sci. Total Environ*. 383: 164–173.

Yao, X., Lau, A.P.S., Fang, M., Chan, C.K. and Hu, M. (2003). Size Distributions and Formation of Ionic Species in Atmospheric Particulate Pollutants in Beijing, China: Inorganic Ions. *Atmos. Environ*. 37: 2991–3000.

Zhang, F., Zhao, J., Chen, J., Xu, Y. and Xu, L. (2011). Pollution Characteristics of Organic and Elemental Carbon in $PM_{2.5}$ in Xiamen, China. *J. Environ. Sci*. 23: 1342–1349.

Zhang, F., Wang, Z.W., Cheng, H.R., Lv, X.P., Gong, W., Wang, X.M. and Zhang, G. (2015). Seasonal Variations and Chemical Characteristics of PM*2.5* in Wuhan, Central China. *Sci. Total Environ*. 518–519: 97–105.

Zhang, R., Jing, J., Tao, J., Hsu, S.C., Wang, G., Cao, J., Lee,

S.L., Zhu, L., Chen, Z., Zhao, Y. and Shen, Z. (2013). Chemical Characterization and Source Apportionment of $PM_{2.5}$ in Beijing: Seasonal Perspective. *Atmos. Chem. Phys*. 13: 7053–7074.

Zhao, P.S., Dong, F., He, D., Zhao, X.J., Zhang, X.L., Zhang, W.Z., Yao, Q. and Liu, H.Y. (2013). Characteristics of Concentrations and Chemical Compositions for $PM_{2.5}$ in the Region of Beijing, Tianjin, and Hebei, China. *Atmos. Chem. Phys.* 13: 4631–4644.

Zhao, X., Zhang, X., Xu, X., Meng, W. and Pu, W. (2009). Seasonal and Diurnal Variations of Ambient $PM_{2.5}$ Concentration in Urban and Rural Environments in Beijing. *Atmos. Environ*. 43: 2893–2900.

Zhao, Q., He, K., Rahn, K.A., Ma, Y., Jia, Y., Yang, F., Duan, F., Lei, Y., Chen, G., Cheng, Y., Liu, H. and Wang, S. (2010). Dust Storm Come to Central and Southwestern China, Too: Implications from a Major Dust Event in Chongqing. *Atmos. Chem. Phys.* 10: 2615–2630.

Zheng, M., Salmon, L.G., Schauer, J.J., Zeng, L., Kiang, C.S., Zhang, Y. and Cass, G.R. (2005). Seasonal Trends in $PM_{2.5}$ Source Contributions in Beijing, China. *Atmos. Environ.* 39: 3967–3976.

Received for review, May 25, 2015
Revised, July 5, 2015
Accepted, July 10, 2015